Effect of the Laser Beam Size on the Cure Properties of a Photopolymer in Stereolithography

Jae-Hyung Sim[1,#], Eun-Dok Lee[2] and Hyeog-Jun Kweon[3]

1 Department of Mechanical and Intelligent Systems Engineering, Pusan National University, Jangjeon 2(i)-Dong, Geumjeong-Gu, Busan, South Korea, 609-735
2 Defects Investigation Office, Korea Automobil Test and Research Institute, 625 Samjon-ri, Songsan-myeon, Hwaseong, Gyeonggi, South Korea, 445-870
3 Department of Ship Building Technology, Sorabol Collage, 165 Chunghyo-Dong, Gyeongju, Gyeongbuk, South Korea, 780-711
Corresponding Author / E-mail: jhsim@pusan.ac.kr, TEL: +82-55-350-5582, FAX: +82-55-354-4011

KEYWORDS : Stereolithography, Processing Parameter, Cured Property, Beam Size, Cure Width, Cure Depth, Surface Roughness

Stereolithography (SLA) is a technique using a laser beam to cure a photopolymer liquid resin with three-dimensional computer-aided design (CAD) data. The accuracy of the prototype, the build time, and the cured properties of the resins are controlled by the SLA process parameters such as the size of the laser beam, scan velocity, hatch spacing, and layer thickness. In particular, the size of the laser beam is the most important parameter in SLA. This study investigated the curing properties of photopolymers as a function of the laser beam size. The cure width and depth were measured either on a single cure line or at a single cure layer for various hatch spacings and laser beam sizes. The cure depth ranged from 0.23 to 0.34 mm and was directly proportional to the beam radius, whereas the cure width ranged from 0.42 to 1.07 mm and was inversely proportional to the beam radius. The resulting surface roughness ranged from 1.12 to 2.23 μm for a ratio of hatch spacing to beam radius in the range 0.5–2.0 at a beam radius of 0.17 mm and a scan velocity of 125 mm/sec.

Manuscript received: July 30, 2007 / Accepted: August 27, 2007

1. Introduction

Rapid prototyping comprises a class of techniques developed to reduce the time to market manufacturing products, and is used by engineers, surgeons, architects, and artists.[1-5] Stereolithography (SLA) is the most widely applied technology and provides outstanding accuracy and surface finish.[6-7]

SLA is a technique that uses a laser beam to solidify a liquid photopolymer in a selective manner for manufacturing prototypes drawn from a computer-aided design (CAD) database. The accuracy and other properties of the prototype are influenced by several factors related to the cured resin.

In general, a prototype manufactured through SLA requires excellent accuracy, the best surface finish, and quick completion. To achieve this, the appropriate process parameters must be selected carefully because a close interrelationship exists among them. The parameters include the size of the laser beam, scan velocity, hatch spacing, and layer thickness.

In particular, the size of the laser beam is an extremely critical factor in achieving the accuracy of the product because it directly impacts the laser power, cure width, and cure depth. The cure width and cure depth should be selected first followed by the hatch spacing and layer thickness.

However, it is relatively difficult to control the size of the laser beam. Therefore, in most previous studies, the accuracy of the product and capacity of machine were evaluated as functions of scan velocity, hatch spacing, and layer thickness, which are relatively easy to control.[8-12] For current SLA machines, the laser beam size is fixed, and only the scan velocity and layer thickness are variable.

This study investigated the cured properties of a photopolymer with different laser beam sizes. The cure width and depth were measured on a single cure line for various laser beam sizes and scan velocities using a purpose-built SLA machine. The cure depth and surface roughness were measured on a single cure line as functions of the laser beam size, hatch spacing, and scan velocity. We used these results to investigate the effects of the size of the laser beam, scan velocity, hatch spacing on surface roughness, and build time for the product. We also suggest potential techniques to improve the capacity of SLA machines.

2. Background

2.1 Laser Beam Size

A photopolymer is a translucent and viscous liquid resin, which solidifies as a result of polymerization caused by exposure to a laser beam. The basic concept of SLA is to manufacture products using photo-cured reactions. To improve accuracy, the laser beam should be focused on a narrow spot.

Laser beams come out of a laser generator with a relatively large diameter, which provides limited spot resolution and weak laser power for curing resin. To overcome this, a SLA machine uses an optical lens to focus the laser beam. As the laser beam diameter decreases, the spot resolution is enhanced, and the laser power

increases as it is concentrated. However, as the size of the laser beam increases, the power of the laser decreases.

Figure 1 shows how the laser beam coming out of the generator is focused through a lens. The beam is not concentrated at a single point, but is gathered at a beam waist with a certain size.

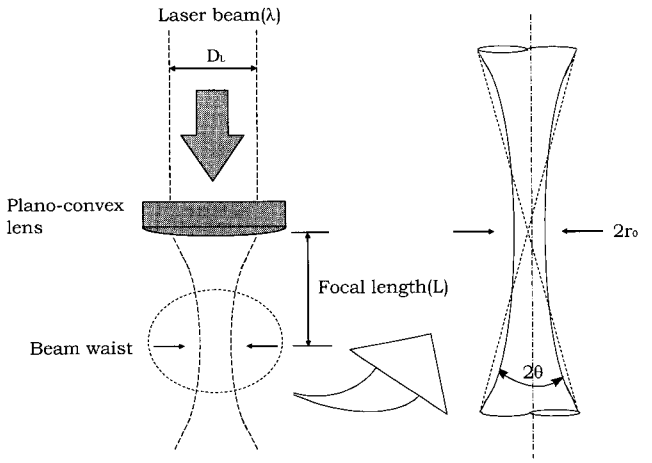

Fig. 1 Focus of the laser beam

The focal radius of laser beam passed through the lens[13] is expressed as

$$r_o = \frac{2\lambda M^2 L}{\pi D_L} \tag{1}$$

where λ is wavelength of the beam, M^2 is the mode purity parameter, L is the focal length of the lens, and D_L is the exposed radius of the laser beam.

In general, the wavelength of the beam, the mode purity parameter, and exposed radius of the laser beam are influenced by the type of laser, while the focal length is determined by the type of lens. This means that the laser beam size can be controlled using lenses with different focal lengths.

2.2 Cured Width and Depth

When laser power is less than a critical value, the photopolymer remains in the uncured liquid state. When the power is greater than the critical value, the photopolymer solidifies through the process of polymerization.[14-16] Figure 2 shows a schematic view of a cure line with the scanning laser beam traveling at constant velocity along the surface of the resin. A single cure line has a Gaussian shape with a maximum depth at the midpoint, very similar to the energy distribution of the laser beam.

The cure width (C_w) and cure depth (C_d) are very important values in manufacturing products. The cure width of a single cure line is calculated as shown in Eq. (2), where P_t is the total laser power, r_0 is the radius of the laser beam, V is the scan velocity, and E_C is the critical exposed energy. The cure width is proportional to the total laser power, and is inversely proportional to the scan velocity and critical exposed energy.

$$C_w = 2r_o\sqrt{\ln\frac{\sqrt{2}P_t}{\pi r_o V E_c}} \tag{2}$$

The cure width is directly related to the determination of hatch spacing and surface roughness. For practical manufacturing, the maximum hatch spacing should be less than the cure width.

The cure depth is calculated as shown in Eq. (3), where D_P is the penetration depth of resin. The cure depth is also proportional to the total laser power, and is inversely proportional to the radius of the laser beam, the scan velocity, and the critical exposed energy.

$$C_d = D_p \ln\frac{\sqrt{2}P_t}{\pi r_o V E_c} \tag{3}$$

The cure depth is directly related to the determination of layer thickness and surface roughness. For practical manufacturing, the thickness of the layer should be less than the cure depth.

Equations (2) and (3) show that the cure width and depth are influenced by processing parameters such as the size of the laser beam, laser power, scan velocity, critical exposed energy, and penetration depth. The critical exposed energy and penetration depth are determined by the laser beam type, the resin type, and the laser beam size gathered through the lens; these are parameters over which the SLA operator has no control. Therefore, the size of the laser beam and the scan velocity are the major factors that determine the cure width and depth.

2.3 Determination of Processing Parameters

The scan velocity, hatch spacing, and layer thickness are very important factors that impact the surface roughness and build time for the product. Therefore, their selection requires care.

In general, as the scan velocity increases, the build time decreases, but when the scan velocity is extremely high, the laser power is insufficient. This results in incomplete solidification, errors, and reduction of surface accuracy. Therefore, the scan velocity should be determined with careful consideration of the resin type, laser power, the cure width, and cure depth.

Based on the scan velocity, the radius of the laser beam (r_o), the cure width (C_w), and hatch spacing (h_s) should be chosen to achieve a good surface finish. If the hatch spacing is too small, solidified spots overlap and are over-cured, and the build time increases. If the hatch spacing is greater than the scan width, the build time decreases, but certain spots may not be exposed to the laser beam and the result is a poor surface finish.

Layer thickness should be selected depending on the cure depth of the solidified resin, which is a function of the scan velocity, as well as the hatch spacing, laser beam size, and surface roughness. When the cure depth is small and cured layers overlap, the layer thickness is greater than the cure depth. When the layer thickness is large, the

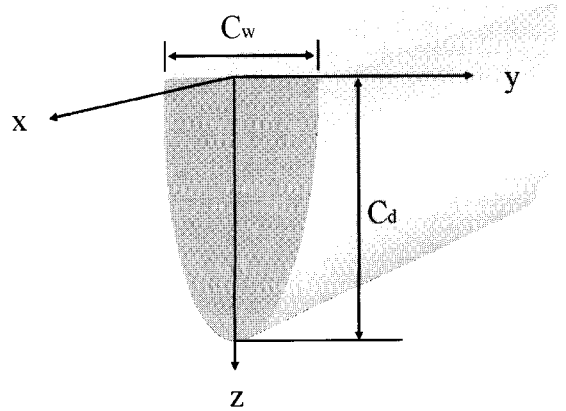

Fig. 2 Schematic representation of a cure line

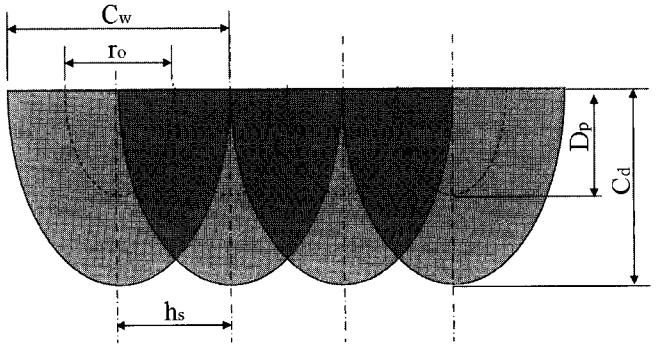

Fig. 3 Schematic representation of a cured layer

build time decreases, but the surface roughness is poor. A reduced layer thickness means an increased number of build layers and increased build time, but good surface roughness.

Overall, a close relationship exists between the accuracy of the product and the processing parameters such as the scan velocity, hatch spacing, and layer thickness. As a result, the parameters should be determined as functions of the laser power.

3. Stereolithography Machine

3.1 Mechanical Parts

We developed a SLA machine in the lab to study the cured properties of photopolymer as a function of the laser beam size.

The lab SLA machine is shown in Fig. 4. The method for exposing the laser beam was the NC table method that determined the exposed spot by moving the XY table. This has excellent spot accuracy compared to the scanning mirror method with the added advantage of constant focus size, regardless of the position of the moving table. Therefore, it was an appropriate method to use in our study.

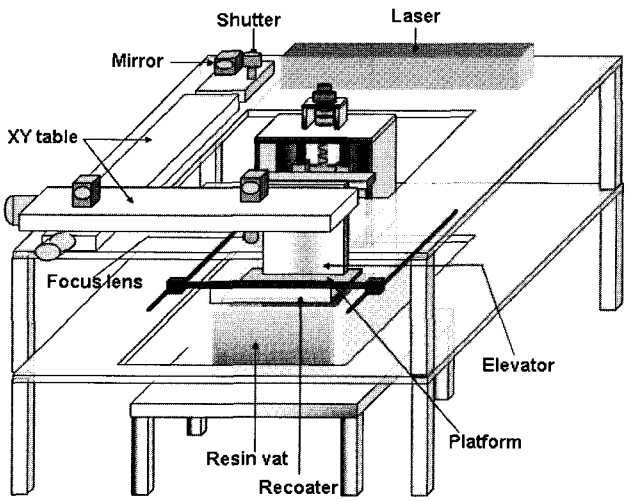

Fig. 4 Lab stereolithography machine

The position and speed of the XY table in the SLA machine are controlled with an AC submotor. The XY table required high scan velocity, minimum shock and mechanical vibration, and outstanding spot accuracy and reproducibility. However, we found that if the scan velocity was too high, shock and shaking occurred. For our experiments, we limited the scan velocity to less than 125 mm/sec.

3.2 Laser Parts

The laser subsystem should maintain a constant focus with a constant spot size, and expose accurately. For our machine, we used three reflecting mirrors, one lens, and a shutter for our laser subsystem.

Out of the generator, the laser beam was directed to the target position on the XY plane by three reflecting mirrors. It was focused on the photopolymer through the lens. The shutter controlled the scan velocity and the beam solidified as a target shape.

Table 1 Laser specifications

Laser type	He–Cd
Wavelength	325 nm
Output power - specified - typical	10 mW 20 mW
Beam radius	0.60 mm
Mode purity parameter (M2)	3.3

The laser beam was a He–Cd with a wavelength of 325 nm. More details on the laser are given in Table 1.

To control the size of the laser beam, we used two lenses with different focal lengths. Table 2 shows the relationship between the focal length and the beam radius.

The beam radius (0.17 and 0.32 mm) in Table 2 was calculated using Eq. (1). For the beam radius of 0.60 mm, the laser beam from the generator reached focus without a lens.

Table 2 Relationship between the focal length and the beam radius

Focal length (mm)	Beam radius (mm)
300	0.17
550	0.32
–	0.60

4. Experiments and Results

4.1 Method and Parameter Determination

We used beam radii of 0.17 mm, 0.32 mm, and 0.60 mm. The photopolymer was type FA-1262A manufactured by SK Chemicals. The size of the laser beam, scan velocity, and hatch spacing were selected as experimental parameters under the control of the operator. However, as dependent variables, the laser power, critical exposed energy, and penetration depth were not controllable. Since the accuracy of the product and the build time was influenced by the three experimental parameters, we measured the cure depth and the surface roughness of the prototype.

For each experimental condition on a single cure line, we actually produced 50 cure lines each 200 nm apart. In each cure line, we randomly selected one spot, and measured the cure depth and width with a Nikon 1-μm resolution transparency meter.

For tests on a single cured layer, we manufactured the test part shown in Fig. 5.

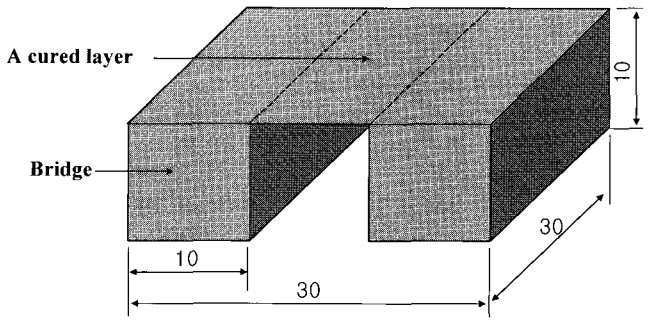

Fig. 5 Test part

The part had right and left bridges with a single layer over the top. Ten test parts were made for each experimental condition. We randomly selected five spots on the single layer between the two bridges and measured the surface roughness at a 90° angle to the scan direction. For this, we used a Mitutoyo SJ-202 surface roughness tester and recorded the surface roughness (Ra) of the middle line. To measure the cure depth, we took a cross section of the middle portion of the test part at 90° to the scan direction, and measured five spots at an interval of 5 mm using the Nikon transparency meter.

Before measuring the results in most of our tests, we cured the resin for 2 h to minimize errors that could be introduced by the post-curing process. The post-curing device had a 20-W UV lamp at each side of a hexagonal chamber to ensure uniform curing.

4.2 Properties of a Single Cure Line

To investigate the cure width and depth as a function of the laser beam size and scan velocity, we conducted an experiment for a single cure line as described in Section 4.1.

The mean and standard deviation of the measured cure width for different beam sizes and scan velocities are shown in Table 3. Figure 6 graphically depicts the cure width as a function of the scan velocity.

For a smaller beam radius, the cure width was reduced across the range of scan velocities. This indicates that the cure width was influenced mainly by the beam radius, as expected from Eq. (2).

Table 3 Mean and standard deviation ($\times 10^{-3}$) for the cure width

Radius \ Velocity		20	40	60	105	125
0.17	mean	0.48	0.44	0.42	0.36	0.34
	σ	1.30	1.31	1.63	1.65	1.71
0.32	mean	0.84	0.80	0.71	0.57	0.53
	σ	1.43	1.44	1.72	1.83	1.93
0.60	mean	1.52	1.32	1.07	–	–
	σ	1.43	1.51	1.79	–	–

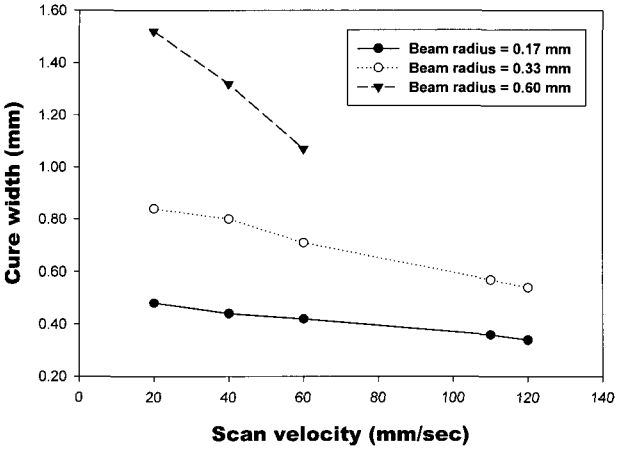

Fig. 6 Cure width vs. scan velocity for various beam sizes

For a fixed beam size, the cure width decreased as the scan velocity increased. However, for a beam radius of 0.60 mm and scan velocities in excess of 60 mm/sec, curing did not occur at all due to insufficient laser power per unit area. For this beam radius, no lens was used, and the beam came straight out of the generator directly onto the surface of the resin.

The slope of the cure width vs. scan velocity curve was dependent on the beam radius. For a radius 0.60 mm, the slope was steep, while it was flat for a radius of 17 mm. As the beam size decreased, the laser power per unit area increased, giving the flat slope. As the beam size increased, the laser power per unit area decreased dramatically, giving a steep slope to the plot of the cure width vs. scan velocity.

The cure width of a single cure line is a critical factor in determining hatch spacing. From our results, for a beam radius of 0.17 mm and a scan velocity of 125 mm/sec, the cure width was 0.34 mm. This means that the hatch spacing should not exceed 0.34 mm. The cure width results are very useful data for determining maximum hatch spacing values.

The mean and standard deviation of the cure depth as a function of beam size and scan velocity are shown in Table 4. Figure 7 graphically depicts the cure depth as a function of scan velocity.

Unlike the results for cure width, the cure depth increased across the whole range of scan velocities, and greater beam radii resulted in a reduced cure depth. This is consistent with Eq. (3), where the laser power per unit area and the depth of penetration increase as the beam radius decreases, resulting in an increase in the cure depth.

For a given beam size, the cure depth was inversely proportional to the scan velocity. For a beam radius of 0.60 mm, and a scan velocity of greater than 60 mm/sec, curing did not occur because the laser power per unit area was too weak.

Table 4 Mean and standard deviation ($\times 10^{-3}$) for the cure depth

Radius \ Velocity		20	40	60	105	125
0.17	mean	0.43	0.38	0.34	0.22	0.20
	σ	1.29	1.34	1.62	1.65	1.69
0.32	mean	0.39	0.33	0.28	0.19	0.18
	σ	1.36	1.47	1.72	1.79	1.88
0.60	mean	0.36	0.29	0.23	–	–
	σ	1.45	1.49	1.79	–	–

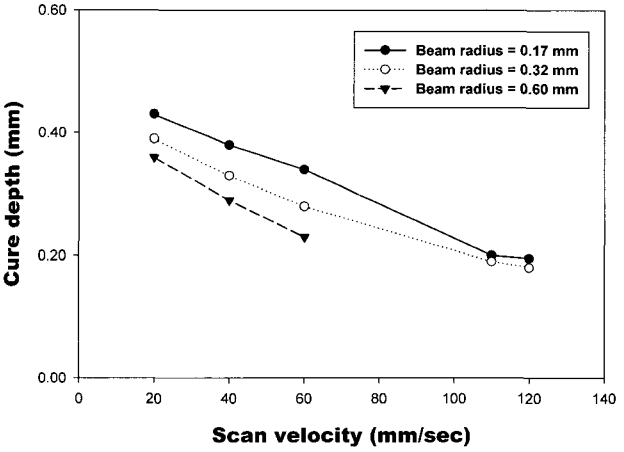

Fig. 7 Cure depth vs. scan velocity for various beam sizes

4.3 Properties of the Single Cure Layer

For a single cure line, the cure depth and surface roughness depended on the beam size and scan velocity, whereas for a single cure layer, they depended on the beam size, scan velocity, and hatch spacing. Therefore, we examined these three factors in the experiment involving a single cure layer.

The mean and standard deviation of the cure depth for different beam radii and scan velocities are shown in Tables 5 and 6. Figures 8 and 9 present the mean cure depths for beam widths of 0.17 mm and 0.32 mm as a function of the scan velocity.

Since curing does not occur at high scan velocities for a beam radius of 0.60 mm, we did not test this condition further.

The results for a single cure layer were similar to those for a single cure line. With the same scan velocity, the cure depth increased as the beam radius decreased, while the cure depth decreased as the scan velocity increased.

However, the absolute cure depth for a single cure layer was greater than that for a single cure line. For example, for a beam radius of 0.17 mm, the cure depth for a single cure layer was 0.38 mm at 40 mm/sec and 0.20 mm at 125 mm/sec, whereas the cure depth for a single cure line was 0.68 mm and 0.47 mm, respectively, for $h_s/r_o = 1.0$.

When the scan velocity was 40 mm/sec and the beam radius was 0.17 mm, the cure width of a single cure line was 0.44 mm, which is greater than the 0.17 mm hatch spacing as Fig. 6 shows. As a result, cured portions overlapped and the laser power per unit area increased, which resulted in an increase in the cure depth.

The cure depth for single cure layer is critical in determining the layer thickness. For $h_s/r_o = 2.0$ and a scan velocity of 125 mm/sec, the cure depth was 0.32 mm, and thus the layer thickness should not exceed 0.32 mm. These results for the cure depth are very useful for determining maximum layer thickness values.

For a given cure depth, increasing the scan velocity reduces the build time and improves the efficiency of the SLA machine. For a beam radius of 0.17 mm and a layer thickness of 0.60 mm, the cure depth was 0.68 mm for $h_s/r_o = 1.0$ and scan velocity of 40 mm/sec and was 0.63 mm at $h_s/r_o = 0.5$ and scan velocity of 125 mm/sec. Both

Table 5 Mean and standard deviation ($\times 10^{-3}$) of the cure depth with a beam radius of 0.17 mm

H_o/r_o \ Velocity		40	60	105	125
0.5	mean	0.86	0.80	0.66	0.63
	σ	1.02	1.09	1.43	1.47
1.0	mean	0.68	0.60	0.49	0.47
	σ	1.16	1.21	1.44	1.47
1.5	mean	0.64	0.57	0.42	0.40
	σ	1.18	1.34	1.45	1.48
2.0	mean	0.61	0.50	0.34	0.32
	σ	1.38	1.47	1.57	1.61

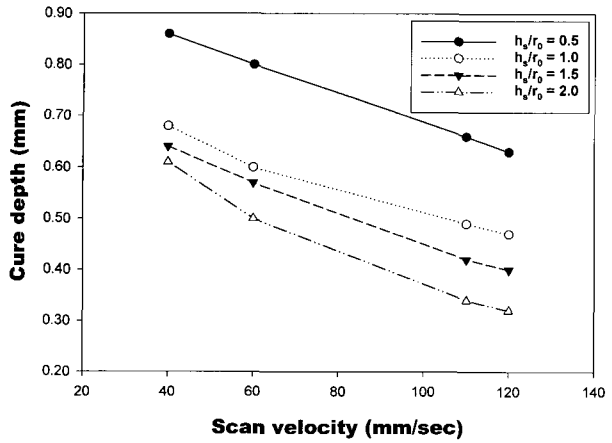

Fig. 8 Cure depth vs. scan velocity for different hatch spacings with a beam radius of 0.17 mm

Table 6 Mean and standard deviation ($\times 10^{-3}$) of the cure depth with a beam radius of 0.32 mm

H_o/r_o \ Velocity		40	60	105	125
0.5	mean	0.78	0.72	0.56	0.54
	σ	1.14	1.29	1.47	1.49
1.0	mean	0.65	0.57	0.44	0.43
	σ	1.27	1.36	1.51	1.54
1.5	mean	0.57	0.49	0.37	0.36
	σ	1.26	1.42	1.51	1.55
2.0	mean	0.53	0.44	0.34	0.32
	σ	1.46	1.52	1.63	1.73

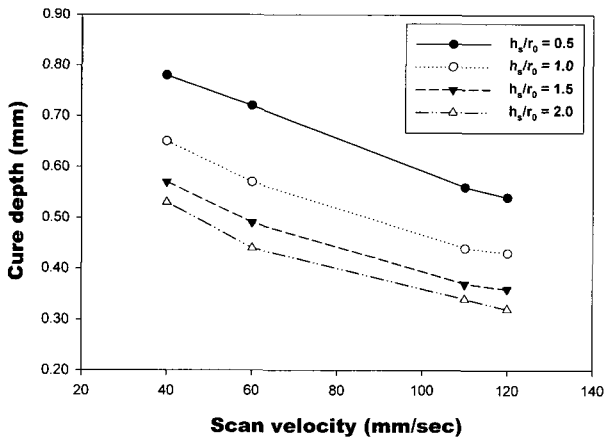

Fig. 9 Cure depth vs. scan velocity for different hatch spacings with a beam radius of 0.32 mm

cases were sufficient to achieve the target layer thickness, but the scan velocity at $h_s/r_o = 0.5$ was 85 mm/sec faster than that at $h_s/r_o = 1.0$. The results suggested that if the ratio of the beam size and scan velocity are controlled appropriately, the build time could be reduced while still achieving the desired cure depth.

The mean and standard deviation of the surface roughness at various ratios of hatch spacing to beam radius for a scan velocity of 125 mm/sec are shown in Table 7.

Regardless of the laser beam size, the surface roughness increased as the ratio of hatch spacing to beam radius increased. However, the difference between the minimum and maximum values was 1.14 μm, well within the tolerance limit for the prototype.

For a hatch spacing of 0.64 mm and a beam radius of 0.32 mm, the build time was half that for a hatch spacing of 0.34 mm and a beam radius of 0.17 mm, even though the ratio of hatch spacing to beam radius is the same for both. Therefore, a beam radius of 0.32 mm and a hatch spacing to beam radius ratio of 2.0 were the most efficient process parameters for the desired surface roughness and build time.

Table 7 Surface roughness as a function of hatch spacing and beam radius for a scan velocity of 125 mm/sec

Beam radius (mm)	h_s/r_o	Surface roughness	
		mean (μm)	σ ($\times 10^{-3}$)
0.17	0.5	1.12	1.25
	1.0	1.55	1.31
	1.5	2.01	1.74
	2.0	2.23	1.83
0.32	0.5	1.33	1.31
	1.0	1.63	1.34
	1.5	2.16	1.76
	2.0	2.47	1.85

5. Conclusions

Based on this study on the cure properties of a photopolymer, the product accuracy, and build time as functions of laser beam size, we drew the following conclusions.

First, for a single cure line, the laser power per unit area decreased as the scan velocity increased, resulting in a decreased cure width and depth.

Second, for a single cure layer, the laser power per unit area decreased as the scan velocity and hatch spacing increased, resulting in a decreased cure depth.

Third, from the experiment on a single cure line, the cure width was 0.34 mm at a 0.17 mm beam radius and 125 mm/sec scan velocity. This meant that the hatch spacing should be less than 0.34 mm to produce cure layers. The maximum hatch spacing could be determined from the cure width measured for each experimental condition.

Fourth, from the experiment on a single cure layer, the measured cure depth was 0.32 mm for a ratio of hatch spacing to beam radius (h_s/r_o) of 2, and a scan velocity of 125 mm/sec. This means that the layer thickness should be less than 0.32 mm. The cure depth measured at each cure layer dictated the maximum layer thickness under each operating condition.

Fifth, the surface roughness of a single cure layer was 2.4 μm at a beam radius of 0.17 mm and 2.23 μm at a beam radius of 0.32 mm with $h_s/r_o = 2.0$. However, the build time for the 0.32 beam radius was half that for the beam radius of 0.17 mm.

Future studies will involve the development of a new SLA machine in which the beam size, scan velocity, hatch spacing, and layer thickness can be controlled automatically based on the data from this study.

REFERENCES

1. Im, Y. G., Cho, B. H., Chung, S. I. and Jeong, H. D., "Development of Build-up Printed Circuit Board Manufacturing Process Using Rapid Prototyping Technology and Screen Printing Technology," International Journal of Precision Engineering and Manufacturing, Vol. 4, No. 4, pp. 51–56, 2003.
2. Hur, S. M. and Lee, S. H., "Study on the Reconstruction of Skull Prototype Using CT Image and Laser Scanner," International Journal of Precision Engineering and Manufacturing, Vol. 1, No. 1, pp. 146–151, 2000.
3. Kim, H. C., Choi, H. T., Lee, H. K. and Lee, S. H., "A Study on Rapid Prototyping Using VRML Model," International Journal of Precision Engineering and Manufacturing, Vol. 3, No. 2, pp. 5–14, 2002.
4. Ahn, D. K. and Lee, S. H., "Improving the Surface Roughness of SL Parts Using a Coating and Grinding Process," International Journal of Precision Engineering and Manufacturing, Vol. 8, No. 3, pp. 14–19, 2007.
5. Yoo, S. R. and Walczyk, D., "An Adaptive Slicing Algorithm for Profiled Edge Laminae Tooling," International Journal of Precision Engineering and Manufacturing, Vol. 8, No. 3, pp. 64–71, 2007.
6. Limaye, A. S. and Rosen, D. W., "Compensation Zone Approach to Avoid Print-though Error in Mask Projection Stereolithography Builds," Rapid Prototyping Journal, Vol. 12, No. 5, pp. 283–291, 2006.
7. Ribeiro Jr, A. S., Hopkinson, N. and Ahrens, C. H., "Thermal Effects on Stereolithography Tools During Injection Moulding," Rapid Prototyping Journal, Vol. 10, No. 3, pp. 176–180, 2004.
8. Zak, G., Haberer, M., Park, C. B. and Benhabib, B., "Mechanical Properties of Short-fiber Layered Composites: Prediction and Experiment," Rapid Prototyping Journal, Vol. 6, No. 2, pp. 107–118, 2000.
9. Li, Y., Li, D. and Lu, B., "Introduction to Stereolithography and its Application," Journal of Applied Optics, Vol. 9, No. 3, pp. 34–36, 1999.
10. Ullett, J. S., Schultz, J. W. and Chartoff, R. P., "Novel Liquid Crystal Resins for Stereolithography—Processing Parameters and Mechanical Analysis," Rapid Prototyping Journal, Vol. 6, No. 1, pp. 8–17, 2000.
11. Yang, Y., Loh, H. T., Fuh, J. Y. H. and Wang, Y. G., "Equidistant Path Generation for Improving Scanning Efficiency in Layered Manufacturing," Rapid Prototyping Journal, Vol. 8, No. 1, pp. 30–37, 2002.
12. Kataria, A. and Rosen, D. W., "Building Around Inserts: Methods for Fabricating Complex Devices in Stereolithography," Rapid Prototyping Journal, Vol. 7, No. 5, pp. 253–262, 2001.
13. Jacobs, P. F., "Rapid prototyping & Manufacturing," Mcgraw-Hill, pp. 71-76, 1993.
14. Pham, D. T. and Ji, C., "Design for Stereolithography," Proceedings of the Institute of Mechanical Engineers, Part C: Journal of Mechanical Engineering Science, Vol. 214, No. 5, pp. 635–640, 2000.
15. Kochan, A., "Rapid Prototyping Gains Speed, Volume and Precision," Assembly Automation, Vol. 20, No. 4, pp. 295–299, 2000.
16. Knitter, R., Bauer, W., GA-hring, D. and Risthaus, P., "RP Process Chains for Ceramic Microcomponents," Rapid Prototyping Journal, Vol. 8, No. 2, pp. 76–82, 2002.